ISBN: 978-3-95450-184-7 doi:10.18429/JACoW-IPAC2018-THPML044

# OPERATION OF A CRYOGENIC CURRENT COMPARATOR WITH NANOAMPERE RESOLUTION FOR CONTINUOUS BEAM INTENSITY MEASUREMENTS IN THE ANTIPROTON DECELERATOR AT CERN

M. Fernandes[1,*], D. Alves, T. Koettig, A. Lees, J.Tan, CERN, Geneva, Switzerland
M. Schwickert, T. Stöhlker[2], GSI, Darmstadt, Germany
C.P Welsch, University of Liverpool, Liverpool, United Kingdom
[1]also at University of Liverpool, Liverpool, United Kingdom
[2]also at Jena University, Jena, Germany

*Abstract*

Low-intensity charged particle beams are particularly challenging for non-perturbative beam diagnostics due to the small amplitude of induced electromagnetic fields. The Antiproton Decelerator (AD) and Extra Low ENergy Antiproton (ELENA) rings at CERN decelerate beams containing $\sim 10^7$ antiprotons. An absolute intensity measurement of the circulating beam is essential to monitor the operational efficiency and to provide important calibration data for the antimatter experiments. This paper reviews the design of an operational Cryogenic Current Comparator (CCC) based on Superconducting QUantum Interference Device (SQUID) for current and intensity monitoring in the AD. Such a system has been operational throughout 2017, relying on a stand-alone cryogenic infrastructure based on a pulse-tube cryocooler. System performance is presented and correlated with different working environments, confirming a resolution in the nanoampere range.

## INTRODUCTION

DC Current Transformers resolution is limited to 1 µA [1]. Other monitors, such as AC Current Transformers or Schottky monitors are able to measure low-intensity beam currents, but neither can simultaneously provide an absolute measurement, with a high current and time resolution, which at the same time is independent of the trajectory and energy.

At CERN's low-energy antiproton ($\bar{p}$) decelerators, the AD and ELENA (currently being commissioned) rings, both bunched and coasting beams of antiprotons circulate with average currents ranging from 300 nA to 12 µA [2]. The AD cycle, shown in Fig. 1, consists of alternate phases of deceleration, when the beam is bunched, and beam cooling, when the beam is debunched and its velocity is kept constant. The beam is also bunched at injection and extraction. In each cycle $5 \times 10^7$ pbar (design value) are injected with a momentum of 3.5 GeV corresponding to a revolution frequency of $f_{\mathrm{rev}} = 1.59$ MHz, and are extracted with $f_{\mathrm{rev}} = 100$ MeV and $f_{\mathrm{rev}} = 174$ kHz. The biggest change in beam current happens at beam injection, when four bunches of length $4\sigma_t = 30$ ns (assuming a Gaussian shape) generate a current slew rate of 8.6 kA s$^{-1}$.

Superconducting QUantum Interference Devices (SQUIDs) based Cryogenic Current Comparator (CCC) monitors have been used to measure DC and slowly extracted beams with resolutions in the nA range by [3, 4]. This project is a collaboration between CERN, GSI, Jena University and Helmholtz Institute Jena.

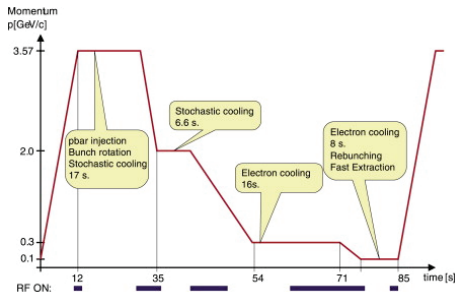


Figure 1: AD cycle. CERN image.

## FUNCTIONING PRINCIPLE OF THE CCC

SQUIDs are highly sensitive magnetic flux sensors that permit the measurement of the weak fields created by the beam. The CCC (schematic shown in Fig. 2) works by measuring the magnetic field induced by a charged particle beam. This field is concentrated in a high-permeability ferromagnetic pickup core, from which it is coupled into the SQUID sensor via a superconducting flux transformer. The measured coupling factor of this circuit $S_{I_b} = \Phi^{\mathrm{in}}/I_b$, where $I_b$ is the beam current and $\Phi^{\mathrm{in}}$ is the magnetic flux coupled to the SQUID through $M_i$, in units of magnetic flux quantum $\phi_0 = 2.068 \times 10^{-15}$ Wb, was $S_{I_b} = 10.49(1)\,\phi_0/\mu$A. The superconducting magnetic shield structure around the pickup-core renders the coupled magnetic field nearly independent of the beam position and also shields the system against external magnetic field perturbations [5,6]. The feedback loop in the SQUID read-out implements a so called Flux Locked Loop (FLL), increasing the dynamic range of the SQUID, but imposing a stability limit on the maximum slew-rate of the input signals [7, 8]. The FLL electronics is configured with a gain of 43 mV/$\phi_0$. The used SQUID/FLL system is supplied by Magnicon [9].

In order to reduce the slew-rate of the signal coupled to the SQUID, a 2nd order RLC low-pass filter has been implemented in the coupling circuit [10]. The coupling function obtained from the current calibration of the monitor after $S_{I_b}(s) = \Phi^{\mathrm{in}}/I_b$ has a bandwidth from DC to 1 kHz and a low frequency gain of $S_{I_b} = 10.49\,\phi_0/\mu$A.

* miguel.fernandes@cern.ch

ISBN: 978-3-95450-184-7 doi:10.18429/JACoW-IPAC2018-THPML044



The CCC is also very sensitive to mechanical and electromagnetic interference, which represent an additional limitation when operating in an accelerator environment.

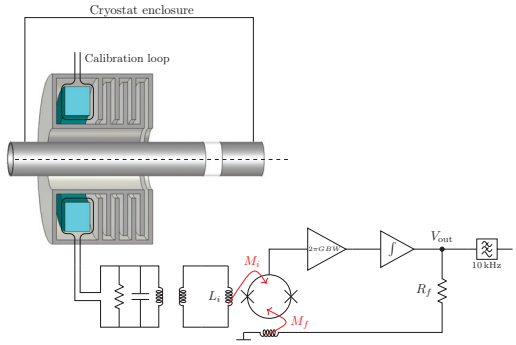


Figure 2: CCC schematic.

## CRYOGENIC SYSTEM

A new cryostat was developed at CERN to house the CCC monitor and to be installed in the AD beam line [11, 12]. The main challenges in cryostat design were: Stand-alone operation at 4.2 K using a pulse-tube cryocooler; Supporting structure optimised for stiffness and to minimise mechanical perturbation of the CCC. Figure 3 shows a diagram of the cryostat's main components. It consists of three main toroidal volumes, which are the external Vacuum Vessel (VV), an intermediate Thermal Shield (TS) and the inner Helium Vessel (HV) which contains the CCC monitor. The beam pipes of the three components are coaxial, with the beam pipe of the VV connecting directly to the beam pipe of the AD ring. Ceramic insulators were required in the beam pipe and in the inner diameter of the HV, to break the path of the beam induced mirror currents that would otherwise highly attenuate the measured magnetic fields down to low-frequencies.

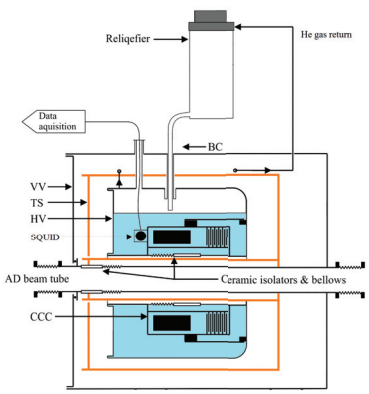


Figure 3: Cryostat and cryocooler. Adapted from [11].

## ACQUISITION SETUP

An automated acquisition and control system was implemented to operate the CCC monitor and synchronize the AD beam measurement acquisition with the AD cycle [13]. This is shown in Fig. 4.

A real-time server, running on the VME-based CPU card, has been developed in order to automate the configuration,

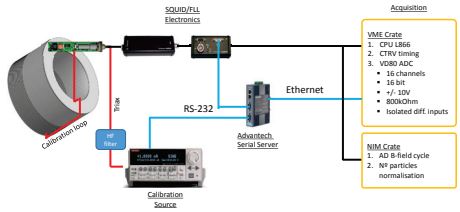


Figure 4: Acquisition system.

calibration, acquisition and publishing of the measurements. The software architecture of this server is based on the CERN Front-End Software Architecture (FESA) C++ framework [14]. The SQUID and the current source are controlled via a serial interface, proxied using a serial device server.The FESA server implements the instruction protocols used to configure and control these devices according to the user settings. A calibration of the monitor is performed at the beginning of each AD cycle, by injecting a known current through the calibration loop in Fig. 2. The measurement is acquired by a 16 bit ADC, with voltage input range of ±10 V and high-impedance differential inputs.

## CURRENT AND INTENSITY MEASUREMENT

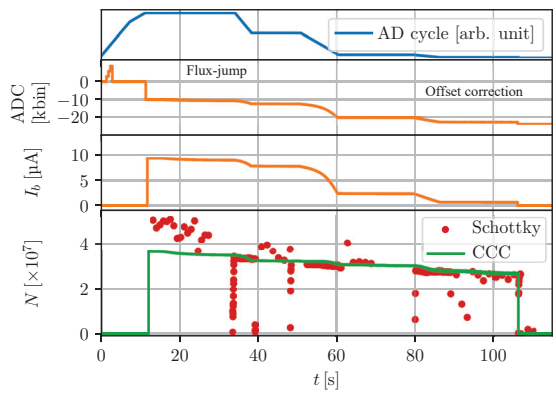


Figure 5: Beam current and intensity measurement.

Figure 5 shows a typical AD cycle measured with the CCC. The top plot shows the AD magnetic cycle; the second plot shows the raw signal acquired by the ADC, where it is observed an offset jump occurring at the moment of beam injection; the third plot shows the corrected and calibrated current measurement; and the bottom plot shows the obtained intensity measurement (number of circulating particles) obtained after normalizing the current measurement against the revolution frequency derived from the magnetic cycle. The intensity measurement is also compared with the Schottky monitor measurement. The flux jump at beam injection is thought to be caused by the interference coming from radio-frequency bunch rotation cavities. Due to this, the absolute measurement offset can only be measured after beam ejection.

The distribution of the obtained current resolution was analyzed for ~ 2500 acquired cycles. Two operational conditions were observed. When the insulation vacuum was

ISBN: 978-3-95450-184-7 doi:10.18429/JACoW-IPAC2018-THPML044

being actively pumped by a roughing pump and a turbo-molecular pump, the observed current resolution values were centered around $\sigma(I_b) \approx 5.5$ nA (reaching a maximum of $\sigma(I_b) \approx 7$ nA), when the pumps were turned off the resolution improves to $\sigma(I_b) \approx 2.8$ nA. This corresponds to an intensity resolution of $\sigma(N) = 1 \times 10^4\,\overline{p}$ at injection energy and $\sigma(N) = 11.1 \times 10^4\,\overline{p}$ at extraction energy.

## BASELINE DRIFTS

The limiting factor to the overall measurement accuracy is not the resolution but errors arising from slow perturbations to the monitor response. Figure 6 shows an example of cycle where no beam has been injected, where it is possible to observe baseline fluctuations. The roughly constant negative slope represents a measurement error of $\Delta I_b \approx 15$ nA. This slope is caused by variation of the helium pressure in the cryostat. From the analysis of multiple cycles where no beam has been ejected it was observed that the maximum drift during an entire cycle was $\Delta I_b \approx 20$ nA. Additionally

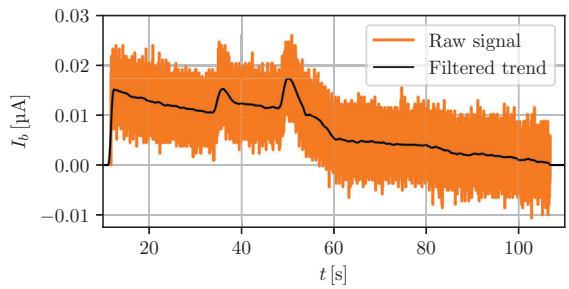


Figure 6: Example of baseline perturbation.

there are other perturbations occurring in the middle of the cycle which were observed to be caused by magnetic cycle of the accelerator. This could be observed by acquiring the monitor output with no beam when the magnets are turned off and when they are being cycled. Figure 7 shows the two examples of such acquisitions where the correlation between the magnetic cycle and monitor output is visible.

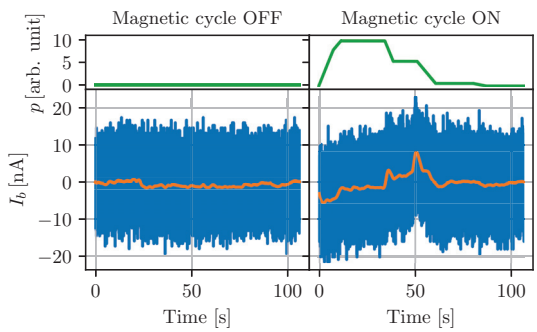


Figure 7: Effect of accelerator magnetic cycle.

However, it is not clear whether this is due to stray magnetic fields picked up by the SQUID or the coupling circuit, or whether this is due to EMI picked up by the FLL electronics or cabling.

## TEMPERATURE VARIATIONS

For a period during 2017 the CCC was cooled by cold helium gas and not liquid. It was observed that the monitor was less sensitive to mechanical vibrations, but the temperature variations which do not normally occur when the monitor is submerged in liquid helium, changed the current sensitivity of the monitor. This changed almost linearly with the temperature, as seen in Fig. 8. However, the correlation is relatively small and equal to $\delta S_{I_b}^{-1}/\delta T = 0.3241$ nA/$\phi_0$/K. For a beam current 10 µA and imposing that the measurement error should be below 10 nA, then the temperature variations should be kept within 300 mK. By having the

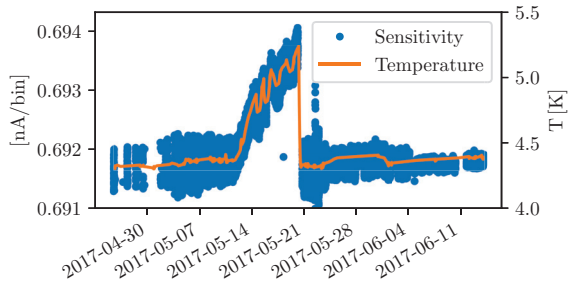


Figure 8: Sensitivity variation as a function of temperature.

CCC temperature actively controlled within such limit could enable a different cooling options, without requiring the use of a liquid helium bath. This could simplify and improve the cryogenic overall availability performance.

## CONCLUSIONS

The developed CCC monitor was operational throughout the majority of 2017 run, providing beam intensity for the AD operations. This is the first fully operational CCC system able to continuously measure both bunched and coasting beams in a synchrotron accelerator. The best obtained current resolution was 2.8 nA, which worsened by a factor $\approx 2$ when the cryostat vacuum pumps were running. This performance was achieved with the cryocooler reliquifier running at the same time, what was only possible due to the careful design of the cryostat to suppress most mechanical vibrations. The limiting factor to the measurement accuracy are slow drifts and perturbations mainly due to pressure variations in the cryostat and the accelerator magnetic cycle. Mitigation of these effects and improvements in the cryogenic system availability are still being implemented, and studies into the development of a similar device for the ELENA decelerator is currently underway.

## ACKNOWLEDGEMENTS

The authors acknowledge the outstanding work of CERN's Central Workshop (EN-MME), Cryogenic group (TE-CRG), Vacuum group (TE-VSC) and AD operations (BE-OP) who assisted in the design, manufacture, assembly and installation of the CCC cryostat. This project has received funding from the European Union's Seventh Framework Programme for research, technological development and demonstration under grant agreement number 289485.

ISBN: 978-3-95450-184-7 doi:10.18429/JACoW-IPAC2018-THPML044



## REFERENCES


[1] P. Odier, "DCCT technology review," C04-12-01.1, Proceedings of CARE-HHH-ABI.

[2] P. Belochitskii *et al*., "The CERN antiproton decelerator (AD) in 2002: status, progress and machine development results," Nuclear Instruments and Methods in Physics Research Section B: Beam Interactions with Materials and Atoms, 214:176 180, 2004. doi:10. 1016/S0168-583X(03)01765-8

[3] A. Peters *et al.*, "A cryogenic current comparator for the absolute measurement of nA beams," BIW98, Standford, May 1998, (p. 163), AIP conference proceedings.

[4] A. Steppke *et al.*, "Application of LTS-SQUIDs in Nuclear Measurement Techniques", IEEE Transactions on Applied Superconductivity, 19(3), 768771, 2009, http://doi.org/10.1109/TASC.2009.2019542

[5] K. Grohmann *et al.*, "Field Attenuation as the Underlying Principle of Cryo Current Comparators," Cryogenics 16(10) (1976) 601.

[6] F. Kurian *et al.*, "Field attenuation of the magnetic shield for a cryogenic current comparator," Proceedings of Beam Instrumentation Workshop, 2012.

[7] D. Drung, "High-performance DC SQUID read-out electronics," Physica C: Superconductivity, Vol. 368, Issues 14, 1 March 2002, 134-140.

[8] R. H. Koch, "Maximum theoretical bandwidth and slewrate of a dc SQUID feedback system," IEEE Transactions on Applied Superconductivity 7(2), p. 3259 (1997).

[9] Magnicon GmbH, "SQUID sensors," datasheet, March 2011.

[10] M. Fernandes *et al.*, "Non-Perturbative Measurement of Low-Intensity Charged Particle Beams," Superconductor Science and Technology, 30(1), 15001, 2017, doi:10.1088/0953-2048/30/1/015001

[11] A. Lees *et al.*, "Design and optimisation of low heat load liquid helium cryostat to house cryogenic current comparator in antiproton decelerator at CERN," IOP Conference Series: Materials Science and Engineering, 171, 12033. doi:10.1088/1757-899X/171/1/012033

[12] A. Lees *et. al.*, "Cryogenic upgrade of the low heat load liquid helium cryostat used to house the Cryogenic Current Comparator in the Antiproton Decelerator at CERN," IOP Conference Series: Materials Science and Engineering, 278, 12193. doi:10.1088/1757-899X/278/1/012193

[13] M. Fernandes *et al.*, "Optimized Cryogenic Current Comparator for CERN's Low-Energy Antiproton Facilities," in Proceedings of IBIC2016, Barcelona, Spain, 2016. doi:10.18429/JACoW-IBIC2016-MOPG48

[14] M. Arruat *et al.*, "Front-End Software Architecture", ICALEPCS 2007.